Pergamon

Vacuum/volume 50/number 1–2/pages 107 to 113/1998

0042–207X/98 $19.00+.00

PII: S0042–207X(98)00032–3

Recent developments in discontinuous metal thin film devices

James E Morris, *Department of Electrical Engineering, State University of New York at Binghamton, NY 13902-6000 USA*

(1) Traditional conduction models for island films on insulating substrates are based on electrostatically activated tunneling, but under-estimate actual conductances by orders of magnitude. A modified model has made significant headway with this problem, as demonstrated by simulations. (2) Strain gauges and gas sensing are briefly discussed as examples of sensor applications based on tunneling between islands. (3) Practical applications are impeded, however, by the difficulty of fabricating reproducible, stable structures, particularly for low TCR films which are the most susceptible to drift. Two efforts to manufacture stable films are described, with emphasis on the reproducibility of one. (4) The simplest discontinuous "film" is the single island coulomb block which forms the basis of the single-electron transistor. Room temperature "SETs" employ chains of islands, i.e. 1-D discontinuous films. © *1998 Elsevier Science Ltd. All rights reserved*

1. Introduction

Discontinuous thin metal films are readily formed in the early stages of nucleation and growth of noble or refractory metal films (Au, Ag, Pt, Pd, W, Mo) on insulating substrates, such as glass (e.g. soda-lime, Corning 7059), alumina, polymers (e.g. polyimides), or cleaved crystal surfaces, typically by physical vapor deposition *in vacuo*. Other processes may be used, the key element being a weak atom–substrate interaction. The films consist of discrete metal islands, of dimensions in the 2–10 nm range, separated by inter-island gaps of 2 nm or more. These parameters can vary considerably with the metal/substrate material system and deposition parameters, especially substrate temperature. Significant electronic conduction is observed in discontinuous films with island diameters and gaps in the 1–10 nm range.[1–4]

The electrical conductance may be expressed as

$$\sigma = \sigma_0 \exp -\delta E/kT,$$

where

$$\delta E = (q^2/4\pi)(r^{-1} - (r+s)^{-1})$$

is the zero field electrostatic energy required to charge a small spherical island of radius, r, by removal of an electron to distance, s, (the inter-island separation), in a medium of dielectric constant ε, q is the electronic charge, k is Boltzmann's constant, T is the absolute temperature, and

$$\sigma_0 = \lambda(4\pi mq^2/h^3B)\cdot(\pi BkT/\sin \pi BkT)\exp -A\phi^{1/2}$$

is the electron tunneling term, with

$$B = \tfrac{1}{2}A\phi^{1/2} \quad \text{and} \quad A = 4\pi s(2m)^{1/2}/h,$$

where h is Planck's constant, and λ, m, and ϕ are the effective tunneling area, electronic mass, and tunneling barrier height. Island size r, increases with average film thickness, and hence δE decreases, (assuming constant deposition conditions). By contrast, gap widths, s, tend to remain constant with thickness, due to a well-defined atomic capture distance around the islands.[2]

2. Contact injection model

Borziak *et al* reported three significant experiments.[5] With previously deposited electrodes, they were able to fabricate discontinuous films with smaller islands and/or wider gaps immediately adjacent to the contacts. These symmetrical "inhomogeneous" films showed that the voltage drop is always greater at the positive end of the film. The second result was the observation of stable and reproducible switching in such films, but the explanation of this effect is a goal of future work, and will not be discussed further here. In the third experiment, the inhomogeneous films were also made asymmetric, i.e. with different inhomogeneous structures at the two electrodes, whereupon the DC resistance became polarity dependent, i.e. it displayed a diode-like effect. These results cannot be explained on the basis of existing conduction models, and indicate that the conduction mechanism must depend significantly upon the islands at the electrodes.[6]

The asymmetric film study has been extended to AC effects.[7] In the traditional model, the film is regarded as a matrix of identical island/gap elements, with the metal island resistance in

series with the parallel combination of gap tunnel resistance R_g and capacitance C_g, where

$$\delta E = \tfrac{1}{2}q^2/C_g.$$

C_g values determined by AC measurements on this model are universally orders of magnitude greater than those consistent with δE. With the asymmetrical inhomogeneous film, two corner frequencies appear, yielding two distinct values for both R_g and C_g, corresponding to the two electrodes. In addition, the C_g values match well to capacitances between the electrodes and film across a single gap width. At extreme asymmetries, a "pseudo-inductive" effect makes an appearance, (as one contact resistance becomes very large), representing a time delay to establish steady-state conductance in the film by charge carrier injection.

The results above lead to the concept of contact injection as the primary source of electrons and holes in the film, with the term "hole" referring to a positively charged island. With zero field, bulk charge separation occurs by tunneling between initially neutral islands, but immediate recombination will commonly follow. Eventually enough charges will drift apart to establish an equilibrium balance between generation and recombination, determined by the Boltzmann distribution. This is the traditional carrier density model which predicts lower conductances than observed. When a voltage is applied to the film, these carriers will begin to drift in the field, and additional carriers will be injected at the electrodes. As the injected carriers drift into the center of the film, the film conductance rises after some time to the steady state value. This is the origin of the pseudo-inductive effect, with the applied field governing the rate of current rise.

The effects above apply to symmetrical film structures, whether homogeneous or inhomogeneous. If one adds the asymmetrical provision, then the different injection probabilities at the positive and negative electrodes produce the diode effect. The "diode" effect requires a quantitative difference in the electronic transfer probabilities at the positive and negative electrodes, a concept supported by the Borziak observation of a higher field at a positively biased electrode than when it is negatively biased.[5] The basis of the difference is shown in Fig. 1, which illustrates energy diagrams for each of the six charge transfer mechanisms. In (a), the three charging processes shown apply to initially neutral islands, whereas in (b) the islands are initially charged, and are neutralized by the electron transfer, and (c) represents the charge "drift" mechanism which dominates transport across the film. In all cases zero field is assumed, and the "films" as shown are electrically neutral. The solid horizontal arrows represent the electron transfer, at the appropriate energy level, and the quadratic tunneling barriers shown include image charge effects. The shaded areas mark equilibrium Fermi levels, and the vertical arrows indicate the δE electrostatic energy level shifts from initial to final Fermi levels in the islands. Electrode Fermi levels are fixed. The electrostatically charge activated injection processes will be the limiting factors in charge transport, and it is immediately apparent that injection tunneling resistance at the negative

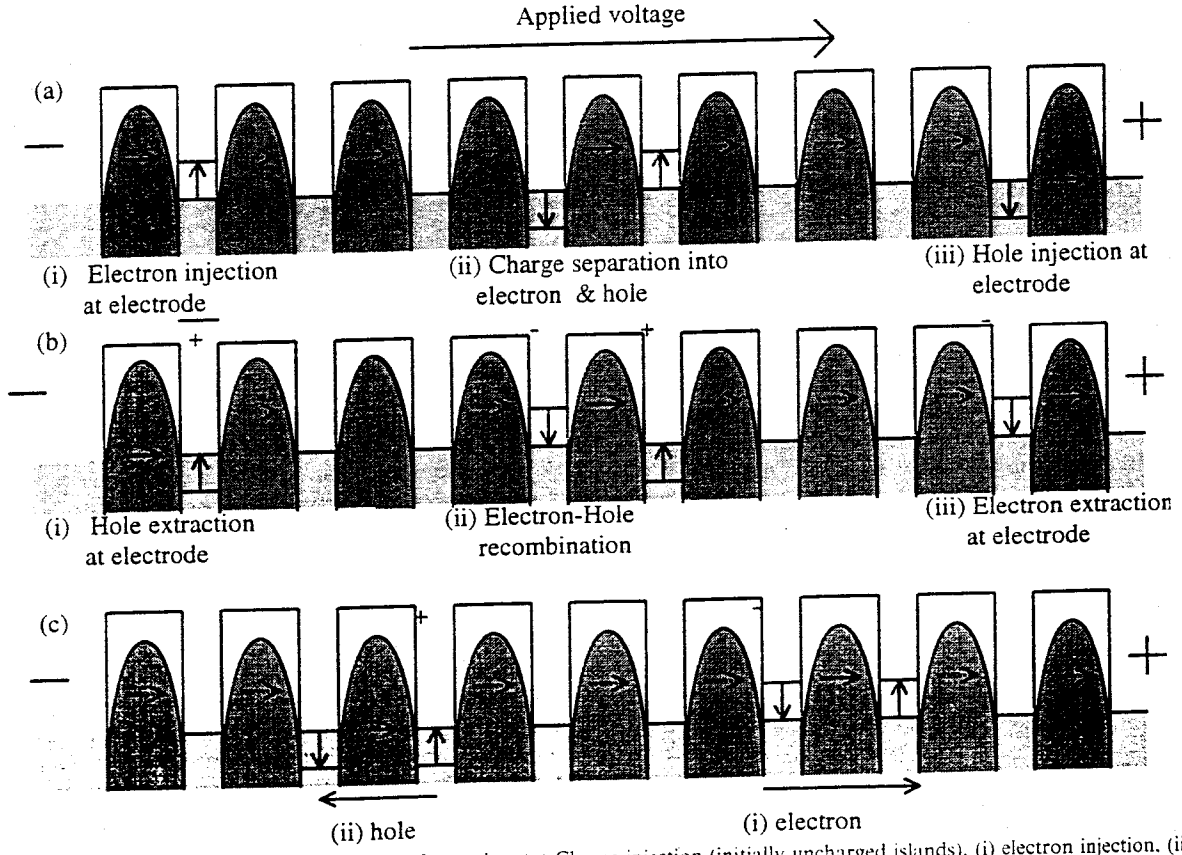

Figure 1. Energy diagrams for electron tunneling transfer modes: (a) Charge injection (initially uncharged islands), (i) electron injection, (ii) charge separation, and (iii) "hole" injection; (b) charge removal (initially charged islands), (i) "hole" removal, (ii) recombination, and (iii) electron removal; and (c) charge transport in the central film (i) electron transfer, and (ii) "hole" transfer.[3] (The island charges shown refer to the initial states before electron transfer.)

electrode is less than that at the positive one. Current continuity will therefore require a higher field at the positive end, and the non-uniform field implies that the film carry a net charge at equilibrium, which will require a finite time to become established.

The electrical behavior of a highly idealized discontinuous thin film has been modeled to verify the concepts developed above by demonstration of the experimental effects described.[8] The results presented below are for a 100×100 array of metal islands on a regular 6 nm square grid. With the exception of the "anomalous" row of 1 nm islands 5 nm from the grounded electrode, all are 3 nm diameter islands separated by 3 nm gaps. The islands are assumed to be spherical for δE calculations, but cubic for the determination of tunneling areas, λ, in σ_0. $T = 300$ K, $\varepsilon_r = 2.5$, and $\phi = 1$ eV. The voltage across the film is $V_{appl} = 10^{-4}$ volts.

To establish initial conditions, the number of equilibrium charged islands is calculated from the Boltzmann distribution, and positive and negative values are assigned randomly in the array. At $t = 0$, voltage is applied and the initial field distribution determined iteratively for the random charge locations. Tunneling probabilities are calculated for all gaps along and across the film, and time is incremented. The probability calculations are repeated at each time increment, and a tunneling transition occurs whenever the accumulated probability exceeds 0.5. The charge separation and recombination processes are simplified: any adjacent positive and negative islands are assumed to immediately recombine, and the underlying Boltzmann distribution reestablished by the random assignment of two charged islands elsewhere. Only the tunneling events in Fig. 1 are considered, (i.e. there are no doubly charged islands), and there is no activation energy associated with the transitions in (b) and (c) where the total system electrostatic energy is unchanged, (i.e. the reduced δE postulated for this case, due to the difference between static and high frequency values of ε, is set to zero).[9]

The diode effect shown in Fig. 2(a) matches the form of Borziak's observation, even to the roughly 10:1 conductance ratio.[5] Superimposed on the I-V characteristic in Fig. 2 are (b) the (log) potential distributions and (c) the charge distributions along the film for negative and positive applied voltages, as defined in the schematics (d). Both field distributions also compare favorably with the general experimental forms (which is more obvious in a linear format). Four separate potential plots along the film are shown for each bias in Fig. 2: (i) the average potential across the film, and the potentials along three individual island columns. There are 100 columns along the film, so (ii) column 2 is one in from one edge, (iii) column 98 is two in from the opposite edge, and (iv) column 50 is in the middle. The greater field curvatures (and fluctuations) along the edges correspond to greater charged island densities than in the middle (due to mutual repulsion between like charges). It is expected that the systematic study of field and charge distributions at higher applied fields will yield a discontinuity and the reproducible switching effect observed in inhomogeneous films. Figure 3 shows the "turn-on" transient, which demonstrates both the pseudo-inductive effect, and the

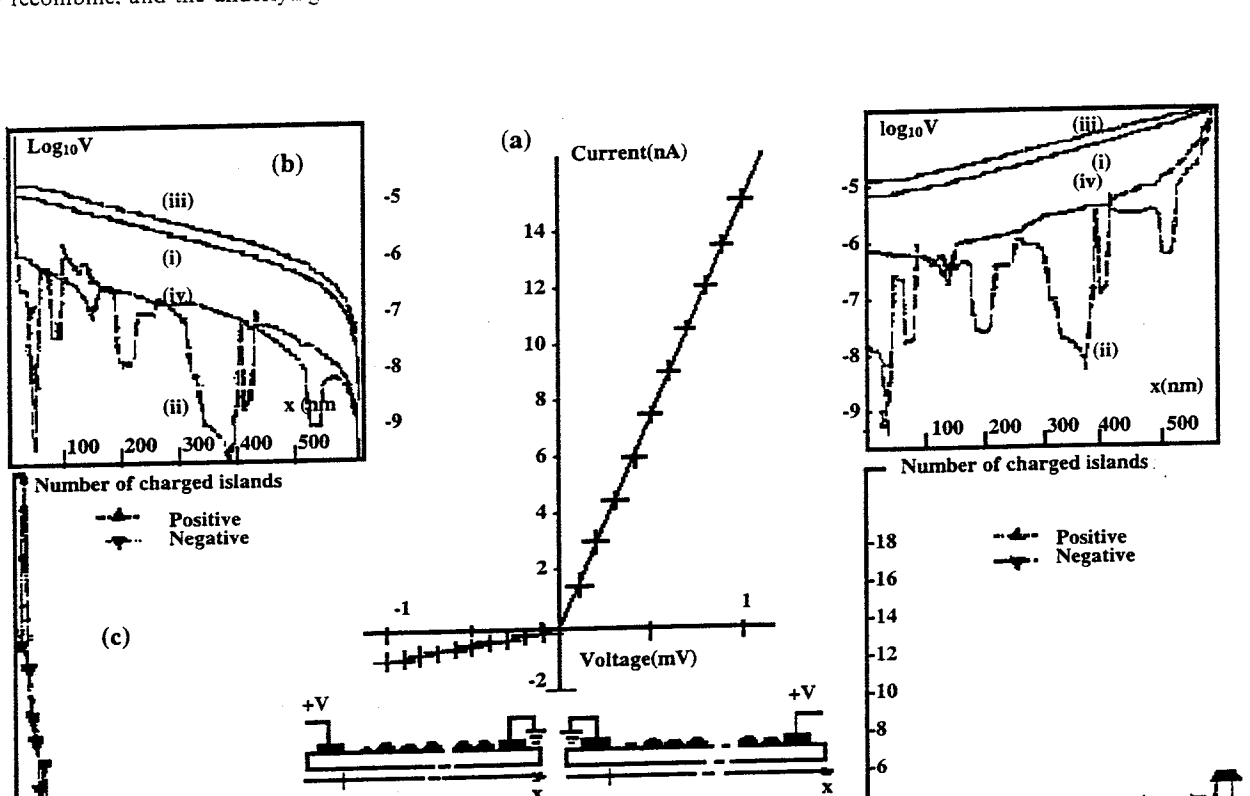

Figure 2. (a) Diode effect, with superimposed (b) potential and (c) charge distributions along the film, with negative and positive biases as defined in schematics (d).[8] (Note position of small island, large gap at left-hand end of film.)

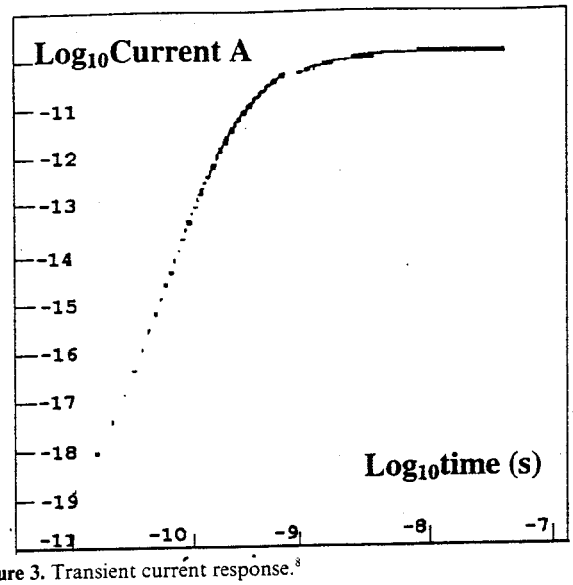

Figure 3. Transient current response.[8]

ratio of final to initial currents. The initial conductance corresponds to the traditional theoretical value based on the equilibrium Boltzmann charge density.

3. Sensors

The exponential dependence of conductivity on tunneling gap width leads to a very high gauge factor for films under stress. The demonstration of strain gauge factors in the range of > 100 drove much of the industrial interest in such systems for commercial applications through the decade 1965–75.[10–12] The problems with the practical implementation of discontinuous film strain gauges are essentially the same as those which limit most other sensor applications. In general, one wants low thermal sensitivity, i.e. δE must be small. This indicates a need for large islands and small gaps, i.e. it puts the film on the edge of coalescence into a semi-continuous filamentary film structure. Such films, however, are particularly unstable following deposition, tending to either agglomerate into large discontinuous islands with large gaps, or to go continuous, with neither predictability nor reproducibility.[13,14] Even less critical discontinuous structures tend to drift irreversibly upwards in resistance following deposition, due to the slow absorption of small islands by large, and the eventual conversion of ellipsoidal islands to the lower energy spheres by surface diffusion.[15] If one cannot achieve low temperature sensitivity, one can compensate by matched devices, but this approach also requires reproducibility and stability (or at least matched drifts).

Discontinuous film resistances are sensitive to ambient gas pressures. The variation of resistance with $(\text{time})^{1/2}$ in air leads to a model based on changes in the tunneling barrier due to gas diffusion into the intervening dielectric.[16] The problem for practical gas sensor applications is that the effect is not gas-specific, although the magnitude of the steady state effect does vary from gas to gas.[2] The Pd/H_2 system is of special interest because of an additional effect. While hydrogen may increase the tunneling barrier due to surface absorption on the palladium islands, diffusion of the hydrogen into solid solution in the bulk increases the palladium lattice constant, leading to increase in island dimensions and a corresponding decrease in tunneling gap width

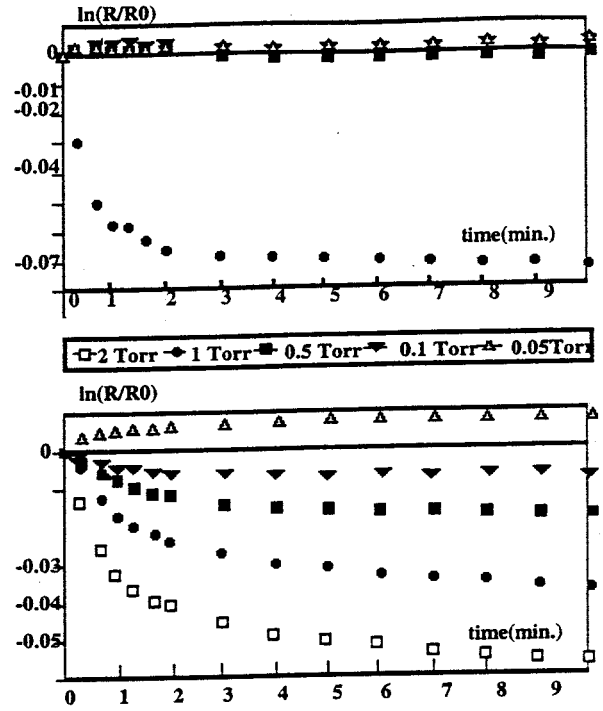

Figure 4. Resistance versus time for 1.6 nm thick discontinuous palladium films when exposed to hydrogen at 300 K for pressures shown.[18]

and film resistance.[17,18] Examples which demonstrate the contributions of both effects are shown in Fig. 4. More systematic study under improved temperature control is necessary to separate the two effects, but it appears as if the potential barrier effect is dominant at low hydrogen partial pressures, until it saturates (if the Pd/H_2 system follows the trends established for gold), and the gap width reduction takes over at higher pressures.[2] To increase sensitivity to the gap width modulation requires small gaps and large islands, i.e. the most unstable and irreproducible structure again.

4. Fabrication

An apparently stable strain gauge has been reported recently, fabricated by ion-plating.[19] In this process, the substrate and growing film are bombarded by low energy neutral particles, with the effect that weakly adherent particles tend to be removed by sputtering, leaving only the more stable components of the film, which are therefore less susceptible to drift and coalescence. The surface ad-atom population between islands, for example, can be assumed to have been fully removed. In addition, the substrate surface bombardment during the very early stages creates defects which act as nucleation centers with greater adhesion to the film atoms than the untreated substrate. A cost of the increased stability is an increased nucleation and island density, which reduces the attainable gauge factor and thermal insensitivity. A maximum gauge factor of 38 at 10 MΩ/square on Kapton-H® polyimide is quoted, less than some reported elsewhere, but on the same order, and an acceptable trade-off for stability.

Now while the ion-plating technique provides the stability necessary for practical applications, it does not yet provide designer control and reproducibility of the structure. Reproducibility comes from the statistical averaging of many random

processes, and can be assessed from the scatter in plots of output parameters, e.g. gauge factor versus resistance. But the irregular nature of the real discontinuous film leads to considerable uncertainty in the comparison of theory and experiment: one can never be sure that the islands observed are typical of those along the actual percolation conduction path. It would be most useful to be able to remove any one (or more) of the random structural variables. To this end it would be advantageous if one could constrain islands to the same size, for example, or to a regular array of sites. Furthermore, if the means of attaching the islands to fixed sites in the latter case was in itself stable, the system might also produce stable films suitable for industrial application.

Scanning Tunneling Microscopy (STM) and/or Atomic Force Microscopy (AFM) technologies provide the means to control island positions. Various techniques have been proposed for applications in similar systems, predominantly on silicon, and follow earlier methods using the electron microscope to fabricate thin metal lines, arrays of metal dots, etc.[20] The difference in the current goal of control of discontinuous film island placement is one of scale. Essentially any means of producing a physical change on the substrate to act as a subsequent nucleation site during deposition can work, e.g. electron polymerization of residual oil vapors to produce a localized carbon deposit. Or, taking advantage of the known preferential nucleation on negative charge sites may be more successful if the charge sites can remain localized for a sufficient length of time.[21] Certainly AFM indentation of soft substrates would be more permanent, but the technique is limited to polymers and may not work on glass or ceramic. If one applies sufficient field to the emission tip, atoms may be stripped from the end as in a field ion microscope. Film deposition by such a technique may be feasible, but is not expected to be practical. However, the properties of chromium as an adhesion promoter for noble metals on substrates such as glass is well known; if one can establish small chromium nucleation sites to act as localized condensation centers in subsequent noble metal deposition, one may also achieve film stability along with reproducibility and structural regularity.

Some initial work has been performed along these lines.[22] A silicon AFM tip has been coated with chromium, and connected to an electrical source. The position of the tip above an insulating substrate (oxidized silicon for the purpose of the test) is controlled by the AFM/STM piezo-electric drive system. In the particular case in question, the probe height was kept constant and the applied voltage was pulsed, but it could be more convenient to apply a fixed potential and reduce the distance to the substrate to exceed the threshold field for emission of chromium atoms from the tip (Fig. 5(a)). Chromium islands have been successfully deposited by the former technique, but much too large at 3 μm in diameter for the intended purpose. Work continues to reduce the chromium island dimensions by reducing the number of atoms deposited, by controlling the discharge current and time (Fig. 5(a)). A 10 nA current (e.g. defined by the diode reverse saturation current) for 10 ns (z-axis pulse) would ideally produce an approximately 3.5 nm diameter hemispherical island, or in practice one somewhat larger if the observation of about three atoms deposited per electron passed persists to low current levels, and more spread due to a substrate contact angle less than $\pi/2$ for strong adhesion. But seed islands of about this dimension on a regular grid would be very appropriate for subsequent deposition of gold or palladium for strain gauge or H_2 sensor applications. The overcoat deposition must be made at a temperature for which the island capture distance for ad-atoms exceeds half the gap between the chromium seed islands (Fig. 5(b)). The chromium islands pin the noble metal islands to the designed location, and for thin overcoats or large seeds also define the island contact dimension (Fig. 5(c)(i)), but in most cases small seeds or thicker overlays will be desired, to ensure control of the film property by the gold, palladium, etc., (Fig. 5(c)(ii)).

5. Single Electron Transistors (SETs)

In discontinuous film conduction theory, the energy required to charge an island as a prerequisite to charge transport is provided randomly by the film's thermal energy. At $T = 0$, there is no such energy source available, and the charging energy must be provided by the applied field itself. The Coulomb block system is the most basic form of discontinuous film, consisting of one single island (Fig. 6(a)), with the property shown in Fig. 6(b) that no current flows below the threshold, conventionally expressed as $qV > \delta E$.[24–27] Clearly, the applied field, F, can similarly provide a portion of the island charging energies at finite temperatures, and this contribution is conventionally included in discontinuous film models by a field reduction of the electrostatic activation energy. In a treatment which exactly parallels Schottky effect theory,[28,29]

$$\delta E = (q^2/4\pi\varepsilon)(r^{-1} - (r+s)^{-1}) - (2r+s)qF$$

at low electric field

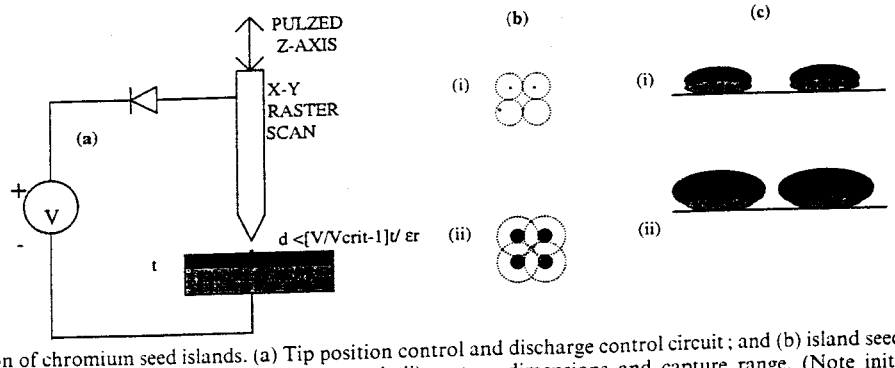

Figure 5. AFM deposition of chromium seed islands. (a) Tip position control and discharge control circuit; and (b) island seed and growth with Au/Pd capture range: (i) seed separations twice the capture range, and (ii) mature dimensions and capture range. (Note initial "interstitial" region.) (c) (i) Thin and (ii) thick over-coating.

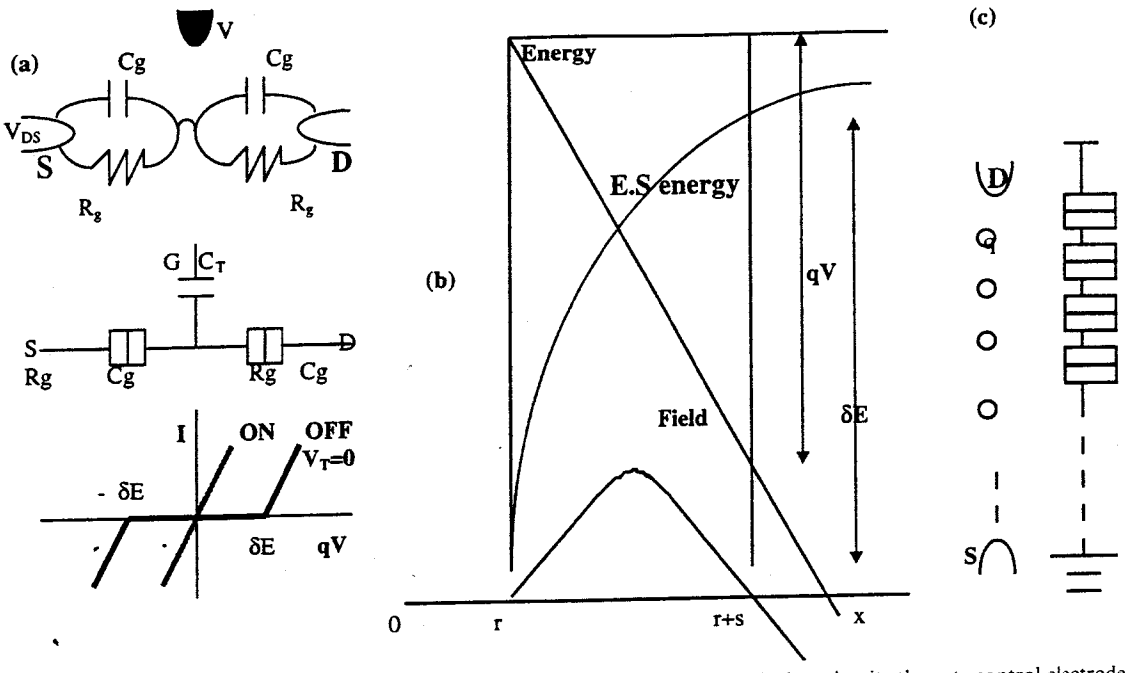

Figure 6. (a) Single island (two tunnel junction) Coulomb Block, with *I-V* characteristic, and equivalent circuit; the gate control electrode to form the SET is shown in half-tone. (b) The electrostatic charging energy barrier (similar to a Schottky barrier) for the case where $qV = \delta E_{V=0}$. (c) The multiple island storage element.

$$F < (q/4\pi\varepsilon)(r+s)^{-2},$$

and

$$\delta E = (q^2/4\pi\varepsilon)r^{-1} + (r/s)(2r+s)qF - 2(q^2/4\pi\varepsilon s)^{1/2}((2r+s)qF)^{1/2}$$

at high field.

$$\delta E \to 0 \quad \text{at } qV = (1+s/r)\delta E_{v=0},$$

i.e. a little higher than usually quoted (Fig. 6(b)). Already such devices have been fabricated for demonstration at low temperatures, and STMs or AFMs are increasingly being used as the accurate nano-fabrication tools.[30–32]

One of the most exciting recent developments in micro electronics has been the development of single electron logic devices from the basic concept of the two terminal Coulomb blockade.[25–27,33–35] The fundamental idea is that the charge can be placed on the island by a third, control electrode, permitting the flow of low voltage current (Fig. 6(a)). The practical problem with the SET concept is to make the devices work at room temperature, or at least $T > 77$ K. To do this, δE must be greater than kT,[34,35] to some specified acceptable probability of random thermal charging, $\exp -(\delta E/kT)$, with the additional benefit that the Coulomb block threshold is also increased. The obvious solution is to reduce island dimensions. A rough calculation for $\delta E \sim 10kT$ at $T = 300$ K, shows that island dimensions of around 1 nm will be necessary taking this approach, i.e. smaller than those demonstrated to date.[34] An alternative approach is to increase $\delta E = q^2/2C$ by decreasing system $C = C_g/n$ for a string of n islands (Fig. 6(c)). One implementation of this concept does not actually use discrete metal islands,[35] but instead allows a percolation channel of nano-crystallites in a polycrystalline silicon film to define the "island" chain. In this case, n is an uncontrollable parameter, but if it is large enough, the fluctuations may be small. Nevertheless, it would be clearly preferable to be able to control the number, size and position of a chain of metal islands for such devices, and this is the goal of the extension of the AFM deposition program described above for the discontinuous film sensors. The intended island dimensions are very different, however, and adequate control of the number of field deposited chromium seed atoms (which must be much less than the total in the noble metal island) may well require SET "turnstile" circuitry.

6. Conclusions

The consistent observation of larger conductances in discontinuous thin films than traditional models predict has been explained by a contact injection model,[8] which also accounts for the diode effect in asymmetric films, and for anomalous AC results, including pseudo-inductance. Renewed interest in sensor applications of discontinuous films is expected to follow the demonstration of structural stability in ion-plated strain gauges.[18] A greater level of structural control is made possible by AFM technology, with both reproducibility and stability achievable. Current research is under way to apply this concept to the fabrication of room temperature SETs.

References

1. Neugebauer, C. A., in *Handbook of Thin Film Technology*, ed. L. I. Maissel and R. Glang, McGraw-Hill, 1970.
2. Kazmerski, L. L. and Racine, D. M., *Journal of Applied Physics*, 1975, **46**, 791.
3. Morris, J. E. and Coutts, T. J., *Thin Solid Films*, 1977, **47**, 3–65.
4. Hill, R. M., *Proceedings of the Royal Society, London, Series A*, 1976, **309**, 397.

5. Borziak, P., Diukov, V., Kostenko, A., Kulyupin, Yu. and Nepijko, S., *Thin Solid Films*, 1976, **36**, 21.
6. Morris, J. E., Mello, A. and Adkins, C. J., in *Physical Phenomena in Granular Materials*, ed. D. Cody, T. H. Geballe and P. Sheng, Materials Research Society Proceedings, MRS Pittsburgh, 1990, **195**, 181–186.
7. Morris, J. E., *Thin Solid Films*, 1990, **193/194**, 110–116.
8. Morris, J. E. and Wu, F., in *Proceedings of 10th International Conference on Thin Films*, Salamanca, Sept., 1996; *Thin Solid Films*, 1997, in press.
9. Leaver, K. D., *J. Phys. C*, 1977, **10**, 249.
10. Parker, R. L. and Krinsky, A., *Journal of Applied Physics*, 1963, **34**, 2000.
11. Boiko, B. T., Palatnik, L. S., Kopach, V. P. and Melent'tev, S. B., *Soviet Physics—Solid State*, 1972, **14**, 1090.
12. Morris, J. E., *Thin Solid Films*, 1972, **11**, 259.
13. Morris, J. E., *Vacuum*, 1972, **22**, 153.
14. Andersson, T., *Journal of Physics D:Applied Physics*, 1976, **9**, 973–985.
15. Morris, J. E., *Thin Solid Films*, 1975, **28**, L21–L23.
16. Morris, J. E., *Thin Solid Films*, 1970, **5**, 339–353.
17. Morris, J. E. and Wu, F., *Thin Solid Films*, 1994, **246**, 17–23.
18. Morris, J. E., Kiesow, A., Hong, M. and Wu, F., *Proc. 5th Int. Workshop Elec. Props. Metal/Non-Metal Microsyst.*, Polanica, 1995; *Int. J. Electronics*, 1996, **81**(4), 441–447.
19. Broitman, E. and Zimmerman, R., *10th International Conference on Thin Films*, Salamanca, Sept., 1996.
20. Pagnia, H., Invited Review. In *Proc. 5th Int. Workshop Elec. Props. Metal/Non-Metal Microsyst.*, Polanica, 1995.
21. Morris, J. E., *Metallography*, 1972, **5**, 41–58.
22. Mueller, F., Hietschold, M. and Morris, J. E., ZfM, Technische Universitat Chemnitz-Zwickau, 1996.
23. Grabert, H. and Devoret, M. H., eds, *Single Charge Tunneling: Coulomb Blockade Phenomena in Nanostructures*, NATO ASI Series B Physics, Vol. 294, Plenum, 1992.
24. Averin, D. V. and Likharev, K. K., *J. Low Temp. Physics*, 1986, **62**, 354.
25. Tucker, J. R., *J. Appl. Phys.*, 1992, **72**, 4399.
26. Ferry, D. K., Barker, J. B. and Jacoboni, C., eds, *Granular Nanoelectronics*, Plenum, 1991.
27. Ahmed, H. and Nakazato, K., *Microelectronic Engineering*, 1996, **32**, 297.
28. Weitzenkamp, L. A. and Bashara, L. M., *Transactions Metallurgical Society AIME*, 1966, **236**, 351.
29. Morris, J. E., *Thin Solid Films*, 1972, **11**, 81–89.
30. Matsumoto, K., *Proc. IEEE*, 1997, **85**(4), 612–628.
31. Servat, J., Gorastiza, P., Sanz, F., Perez-Murano, F., Barniol, N., Abagal, G. and Aymerich, X., *J. Vac. Sci. Technol A.*, 1996, **14**(3), 1208–1212.
32. Perez-Murano, F., Abagal, G., Barniol, N., Aymerich, X., Servat, J., Gorastiza, P. and Sanz, F., *J. Appl. Physics*, 1995, **78**, 6797–6801.
33. Nakazato, K., Blaikie, R. J., Cleaver, J. R. A. and Ahmed, H., *Electronics Lett.*, 1993, **29**(4), 384.
34. Rosner, W., Hofmann, F., Vogelsang, T. and Risch, L., *Microelectronic Engineering*, 1995, **27**, 55–58.
35. Yano, K., Ishii, T., Hashimoto, T., Kobayashi, T., Marai, F. and Seki, K., *IEEE Trans. Electron Devices*, 1994, **41**, 1628.